Structure and Reactivity of Vinylcyclopropane Radical Cation: Electron Transfer Photochemistry and *ab Initio* Calculations

Torsten Herbertz and Heinz D. Roth*

Contribution from the Department of Chemistry, Rutgers University, Wright-Rieman Laboratories, New Brunswick, New Jersey 08855-0939

Received February 2, 1998

Abstract: The electron-transfer photochemistry of vinylcyclopropane (**1**) generates three ring-opened products, **2**−**4**, each bearing a methoxy as well as a 4-cyanophenyl group. The products are ascribed to nucleophilic attack of methanol on the radical cation, $\mathbf{1}^{\bullet+}$. The attack is regioselective but not regiospecific; attack at the secondary cyclopropane carbons, leading to **2** and *trans*-**3**, is preferred; attack at the terminal vinylic carbon, yielding *trans*-**4**, occurs to a lesser extent. The potential surface of $\mathbf{1}^{\bullet+}$ was probed by ab initio calculations; $\mathbf{1}^{\bullet+}$ has two minima, *anti*- and *syn*-$\mathbf{1}^{\bullet+}$; both have C_s symmetry and belong to the unusual structure type with two lengthened cyclopropane bonds. The calculations are in general agreement with the observed reaction pattern.

Introduction

Radical cations of molecules containing strained ring moieties as well as olefinic fragments have been the focus of much interest in recent years;[1] the conjugative and homoconjugative interactions between the two functions have been probed in detail: changes in molecular geometry caused by one-electron oxidation have been delineated for various substrates and the spin and charge density distributions in the resulting radical cations have been assessed.[2] Typically, the reactions of these species proceed with release of ring strain;[3−6] in some systems, ring opening is assisted by a nucleophile.[7,8]

Vinylcyclopropane radical cation, $\mathbf{1}^{\bullet+}$, the simplest radical cation containing an olefinic moiety and a cyclopropane ring, has not been characterized adequately, although several derivatives have been studied recently.[6,9−12] In the gas phase, the molecular ion, $\mathbf{1}^{\bullet+}$, rearranges to the penta-1,3-diene radical cation.[9] Related rearrangements have been documented for two rigidly linked vinylcyclopropane systems in solution: the electron-transfer-induced rearrangements of sabinene to β-phellandrene, and of α-thujene to α-phellandrene, were interpreted as novel examples of sigmatropic shifts in radical cations.[10b]

The spin density distributions of several derivatives of $\mathbf{1}^{\bullet+}$, in which the two functionalities are locked in either the anti (viz., sabinene) or syn orientation (bicyclo[3.1.0]hex-2-ene, bicyclo[4.1.0]hept-2-ene, α- and β-thujene), were characterized by CIDNP studies.[10c,12a] Theoretical approaches include an early STO-3G calculation for $\mathbf{1}^{\bullet+}$ with a seriously restricted geometry[11a] and more recent INDO calculations.[11b,c] In addition, two conformers of the 2-carene radical cation were calculated

(1) (a) Forrester, R. A.; Ishizu, K.; Kothe, G.; Nelsen, S. F.; Ohya-Nishiguchi, H.; Watanabe, K.; Wilker, W. Organic Cation Radicals and Polyradicals. In *Landolt Börnstein, Numerical Data and Functional Relationships in Science and Technology*; Springer-Verlag: Heidelberg, 1980; Vol. IX, Part d2. (b) Yoshida, K. *Electrooxidation in Organic Chemistry: The Role of Cation Radicals as synthetic Intermediates*; Wiley: New York, 1984. (c) Shida, T. *Electronic Absorption Spectra of Radical Ions*; Elsevier: Amsterdam, 1988. (d) *Radical Ionic Systems*; Lund, A., Shiotani, M., Eds.; Kluwer Academics: Dordrecht, 1991. (e) Roth, H. D. *Top. Curr. Chem.* **1992**, *163*, 133.

(2) (a) Ledwith, A. *Acc. Chem. Res*. **1972**, *5*, 133. (b) Shida, T.; Haselbach, E.; Bally, T. *Acc. Chem. Res.* **1984**, *17*, 180−186. (c) Nelsen, S. F. *Acc. Chem. Res.* **1987**, *20*, 269−276. (d) Roth, H. D. *Acc. Chem. Res*. **1987**, *20*, 343−350. (e) Bauld, N.; Bellville, D. J.; Harirchian, B.; Lorenz, K. T.; Pabon, R. A.; Reynolds, D. W.; Wirth, D. D.; Chiou, H.-S.; Marsh, B. K. *Acc. Chem. Res*. **1987**, *20*, 371. (f) Yoon, U. C.; Mariano, P. S. *Acc. Chem. Res.* **1992**, *25*, 233. (g) Gerson, F. *Acc. Chem. Res*. **1994**, *27*, 63. (h) Mirafzal, G. A.; Liu, J.; Bauld, N. *J. Am. Chem. Soc*. **1993,** *115*, 6072.

(3) Quadricyclane to norbornadiene radical cation: (a) Roth, H. D.; Schilling, M. L. M.; Jones, G., II *J. Am. Chem. Soc*. **1981**, *103*, 1246−1248. (b) Roth, H. D.; Schilling, M. L. M. *J. Am. Chem. Soc*. **1981**, *103*, 7210−7217.

(4) Methylenecyclopropane rearrangement: (a) Takahashi, Y.; Mukai, T.; Miyashi T. *J. Am. Chem. Soc.* **1983**, *105*, 6511−6513. (b) Miyashi, T.; Takahashi, Y.; Mukai, T.; Roth, H. D.; Schilling, M. L. M. *J. Am. Chem. Soc.* **1985**, *107*, 1079−1080.

(5) Bicyclobutane to cyclobutene rearrangement: (a) Gassman, P. G.; Hay, B. A. *J. Am. Chem. Soc.* **1985**, *107*, 4075. (b) Gassman, P. G.; Hay, B. A. *J. Am. Chem. Soc.* **1986**, *108*, 4227. (c) Arnold, A.; Burger, U.; Gerson, F.; Kloster-Jensen, E.; Schmidlin, S. P. *J. Am. Chem. Soc.* **1993**, *115*, 4271−4281.

(6) Vinylcyclopropane rearrangement: (a) Dinnocenzo, J. P.; Schmittel, M. *J. Am. Chem. Soc*. **1987**, *109*, 1561−1562. (b) Dinnocenzo, J. P.; Conlon, D. A. *J. Am. Chem. Soc*. **1988**, *110*, 2324−2326.

(7) Cyclopropane systems: (a) Rao, V. R.; Hixson, S. S. *J. Am. Chem. Soc.* **1979**, *101*, 6458. (b) Mizuno, K.; Ogawa, J.; Kagano, H.; Otsuji, Y. *Chem. Lett.* **1981**, 437−438. (c) Mizuno, K.; Ogawa, J.; Otsuji, Y. *Chem. Lett*. **1981**, 741−744. (d) Mazzocchi, P. H.; Somich, C.; Edwards, M.; Morgan, T. Ammon, H. L. *J. Am. Chem. Soc*. **1986**, *108*, 6828. (e) Dinnocenzo, J. P.; Todd, W. P.; Simpson, T. R.; Gould, I. R. *J. Am. Chem. Soc*. **1990**, *112*, 2462−2464. (f) Hixson, S. S.; Xing, Y. *Tetrahedron Lett.* **1991**, *32*, 173−174. (g) Dinnocenzo, J. P.; Lieberman, D. R.; Simpson, T. R. *J. Am. Chem. Soc*. **1993**, *115*, 366−367.

(8) Bicyclobutane systems: (a) Gassman, P. G.; Olson, K. D.; Walter, L.; Yamaguchi, R. *J. Am. Chem. Soc*. **1981**, *103*, 4977. (b) Gassman, P. G.; Olson, K. D. *J. Am. Chem. Soc*. **1982**, *104*, 3740.

(9) Dass, C.; Peake, D. A.; Gross, M. L. *Org. Mass. Spectrom.* **1986**, *21*, 741−746.

(10) (a) Weng, H.; Sethuraman, V.; Roth, H. D. *J. Am. Chem. Soc*. **1994**, *116*, 7021. (b) Weng, H.; Sheik, Q.; Roth, H. D. *J. Am. Chem. Soc.* **1995**, *117*, 10655−10661. (c) Roth, H. D.; Weng, H.; Herbertz, T. *Tetrahedron* **1997**, *53*, 10051−10070.

(11) (a) Scott, L. T.; Erden, I.; Brunsvold, W. R.; Schultz, T. H.; Houk, K. N.; Paddon-Row, M. N. *J. Am. Chem. Soc*. **1982**, *104*, 3659−3664. (b) Shchapin, I. Yu.; Fel'dman, V. I.; Belevskii, V. N.; Donskaya, N. A.; Chuvylkin, N. D. *Russ. Chem. Bull.* **1994**, *43*, 1−12. (c) Shchapin, I. Yu.; Fel′dman, V. I.; Belevskii, V. N.; Donskaya, N. A.; Chuvylkin, N. D. *Russ. Chem. Bull*. **1995**, *44*, 203−227.

(12) (a) Roth, H. D.; Herbertz, T. *J. Am. Chem. Soc*. **1993**, *115*, 9804−9805. (b) Arnold, D. R.; Du, X.; de Lijser, H. J. P. *Can. J. Chem.* **1995**, *73*, 522.

10.1021/ja980367s CCC: $15.00 © 1998 American Chemical Society
Published on Web 11/05/1998

recently, also at the STO-3G level.[12b] Finally, several 2-*p*-anisyl derivatives undergo electron-transfer-induced vinylcyclopropane rearrangements.[6]

In this paper, we report a dual approach to the parent vinylcyclopropane radical cation. We have studied the electron-transfer photochemistry of **1**; the photoreaction generates the radical cation, **1**$^{\bullet+}$, which reacts by nucleophilic capture. The product distribution reveals the point of attack by the nucleophile and may yield information on how the charge is distributed in the radical cation. To supplement the experimental study, we performed ab initio calculations (extended basis sets and electron correlation to UMP4(SDQ)/6-31G*) on the potential energy surface of **1**$^{\bullet+}$.[13−15] The calculated radical cation minima are compared with minima on the parent potential surface, either calculated or based on a wide range of experimental studies. Further, we modeled the regiochemistry of nucleophilic addition to *anti*-**1**$^{\bullet+}$ by ab initio methods (UHF). For these calculations, we placed a CH_3OH molecule within 2.5 Å of fully optimized *anti*-**1**$^{\bullet+}$; the progress of the reaction was probed by transition state geometry optimization, including frequency analyses of the extrema.

Vinylcyclopropane Potential Surface. To provide an appropriate background for the structure of **1**$^{\bullet+}$, we review briefly pertinent experimental results for **1**. The conformational aspects of **1** have been studied in significant detail by an extensive range of experimental techniques as well as calculations. The neutral parent has several rotational conformers relative to the bond connecting the vinyl and cyclopropane functions. X-ray diffraction shows that **1** crystallizes as the *anti* conformer.[16] In the gas phase and in solution, on the other hand, more than one conformer is present. Electron diffraction[17] and vibrational,[18] Raman,[19] and NMR spectroscopy[20] support a rapid equilibrium between the anti and a lesser conformer. Electron diffraction results support a 3:1 mixture ($\Delta E = 1.1$ kcal/mol) of these conformers and a torsion angle of ∼55° for the gauche conformer.[17b]

NMR studies of **1** and derivatives have been interpreted in terms of a two-well potential surface, with minima at the syn and anti geometries,[20a] or a three-well potential surface, with minima at the anti and two gauche geometries.[20b] The temperature dependence of coupling constants (J), chemical shifts and, particularly, the line intensities are best accommodated by the three-well potential surface.[20b] Temperature-dependent changes in the Raman spectrum are compatible with both trans and gauche conformers as minima; they suggest an enthalpy difference, $\Delta H \sim 1.4$ kcal/mol, between the two conformers and a barrier, $\Delta H^{\ddagger} \sim 4$ kcal/mol.[19]

The potential energy surface of **1** has been examined also by computational means.[21] Calculations with limited basis sets (STO-3G) suggested a four-well potential surface, with the s-cis conformer as a shallow minimum between a pair of gauche conformers, $\Delta H \sim 0.4$ kcal/mol, and a barrier, $\Delta H^{\ddagger} \sim 0.1$ kcal/mol.[21a] Expanded split-valence basis sets (4-31G or higher) yielded a three-well surface, on which trans and gauche conformers are minima ($\Delta H \sim 1.2$ kcal/mol; $\Delta H^{\ddagger} \sim 3$ kcal/mol, barrier between s-trans and gauche) and the s-cis conformer was a saddle point ($\Delta H^{\ddagger} \sim 1.5$ kcal/mol above the gauche conformers).[21d] These assignments are confirmed by the high-level ab initio calculations reported here.

Experimental Section

Materials. Vinylcyclopropane was synthesized according to Hudlicky and Tsunoda[22] by a modified Wittig reaction from cyclopropane carboxaldehyde (Aldrich, 99%) and methyltriphenylphosphonium bromide (Aldrich, 98%) in ∼70% yield. Both reagents were used as received. 1,4-Dicycanobenzene (Aldrich, 98%) was purified by recrystallization from absolute ethanol; phenanthrene (Aldrich, 98%) was recrystallized from *n*-hexane. Acetonitrile (Fischer, A.C.S. certified) was distilled under nitrogen from calcium hydride immediately prior to the photoreaction; methanol (Fischer, Spectranalyzed) was used as received.

Photoreactions. A solution containing 2.56 g (0.25 M) of 1,4-dicyanobenzene and 0.89 g (0.063 M) of phenanthrene in 80 mL of acetonitrile/methanol (3:1 by volume) was placed in a 30-mm i.d. tube and purged with nitrogen for 15 min. The tube was sealed with a rubber septum, 1.7 mL (∼0.25 M) of vinylcyclopropane was injected, and the mixture was cooled to −10 °C (central cooling finger) and irradiated in a Rayonet RPR-100 photoreactor equipped with 16 RPR-3500 lamps. The reaction progress was monitored by gas chromatography on a GC/MS system (HP 5890 series II Plus GC interfaced with a HP 5972 mass selective detector), using a 30 m × 0.25 mm × 0.25 μm HP-5 capillary column (cross-linked methyl silicone on fused silica).

Isolation of Products. Reaction products were isolated by liquid column chromatography, using a set of 50-cm columns with inside diameters ranging from 1 to 5 cm. The columns were packed with ∼100 g of silica gel (200−400 mesh, E. M. Science); the evaporated reaction mixture, adsorbed on ∼3 g of silica gel, was added to the column and eluted with solvents or solvent mixtures of gradually changing composition, usually from light petroleum ether (bp < 65 °C) to mixtures with methylene chloride or ethyl acetate. A total of 3 passes were required to isolate the products.

Characterization of Products. The structures of the isolated products were assigned on the basis of MS and NMR data. Proton NMR spectra were recorded on a Varian Gemini-200 spectrometer; ^{13}C spectra were recorded on the Varian Gemini-200 spectrometer operating at 50.3 MHz. The structural features were derived from 1D ^1H, 2D COSY, 1D ^{13}C, and DEPT, where appropriate.

Calculational Methods. Calculations were carried out with the GAUSSIAN 94 series of electronic structure programs,[14] using extended basis sets, including d-type polarization functions on carbon (6-31G*). Full geometry optimization and frequency analyses for the vinylcyclopropane parent (restricted, i.e., RHF and RMP2) and radical cation (unrestricted, i.e., UHF, UB3LYP and UMP2) were carried out both

(13) A detailed description of the theoretical methods used in this work is contained in the following: Hehre, W. J.; Radom, L.; Pople, J. A.; Schleyer, P. v. R. *Ab Initio Molecular Orbital Theory*; Wiley-Interscience, New York, 1986.

(14) Frisch, M. J.; Trucks, G. W.; Schlegel, H. B.; Gill, P. M. W.; Johnson, B. G.; Robb, M. A.; Cheeseman, J. R.; Keith, T.; Peterson, G. A.; Montgomery, J. A.; Raghavachari, K.; Al-Laham, M. A.; Zakrzewski, V. G.; Ortiz, J. V.; Foresman, J. B.; Peng, C. Y.; Ayala, P. Y.; Chen, W.; Wong, M. W.; Andres, J. L.; Replogle, E. S.; Gomperts, R.; Martin, R. L.; Fox, D. J.; Binkley, J. S.; DeFrees, D. J.; Baker, J. P.; Stewart, J. P.; Head-Gordon, M.; Gonzalez, C.; Pople, J. A. *GAUSSIAN 94*; Gaussian, Inc.: Pittsburgh, PA.

(15) (a) Eriksson, L. A.; Malkin, V. G.; Malkina, O. L.; Salahub, D. R. *J. Chem. Phys.* **1993**, *99*, 9756−9763. (b) Eriksson, L. A.; Malkin, V. G.; Malkina, O. L.; Salahub, D. R. *Int. J. Quantum Chem.* **1994**, *52*, 879−901. (c) Batra, R.; Giese, B.; Spichty, M.; Gescheidt, G.; Houk, K. N. *J. Phys. Chem.* **1996**, *100*, 18371−18379.

(16) (a) Nijveldt, D.; Vos, A. *Acta Crystallogr.* **1988**, *B44*, 281−289. (b) Nijveldt, D.; Vos, A. *Acta Crystallogr.* **1988**, *B44*, 289−296. (c) Nijveldt, D.; Vos, A. *Acta Crystallogr.* **1988**, *B44*, 296−307.

(17) (a) de Meijere, A.; Lüttke, W. *Tetrahedron* **1969**, *25*, 2047−2058. (b) Traetteberg, M.; Bakken, P.; Almeningen, A.; Lüttke, W. *J. Mol. Struct.* **1988**, *189*, 357−371.

(18) Codding, E. G.; Schwendeman, R. H. *J. Mol. Spctrosc.* **1974**, *49*, 226−231.

(19) Carreira, L. A.; Towns, T. G.; Malloy, T. B., Jr. *J. Am. Chem. Soc.* **1978**, *100*, 385−388.

(20) (a) Lüttke, W.; de Meijere, A. *Angew. Chem., Int. Ed. Engl.* **1966**, *5*, 512−513. (b) De Mare, G. R.; Martin, J. S. *J. Am. Chem. Soc.* **1966**, *88*, 5033−5034. (c) For a thorough discussion of the ^1H NMR spectrum of **1**, see: Schrumpf, G. *Tetrahedron Lett.* **1970**, 2571−2574.

(21) (a) Hehre, W. J. *J. Am. Chem. Soc.* **1972**, *94*, 6592−6597. (b) Skancke, A.; Boggs, J. E. *J. Mol. Struct., Theochem.* **1979**, *25*, 267−274. (c) Mare, G. R.; Peterson, M. R. *J. Mol. Struct., Theochem.* **1982**, *89*, 213−225. (d) Klahn, B.; Dyczmons, V. *J. Mol. Struct., Theochem.* **1985**, *122*, 75−94.

(22) Hudlicky, T.; Tsunoda, T. *Synlett* **1990**, 322.

with and without imposed symmetry; both approaches lead to essentially the same minima (C_s point group); subsequent energy comparisons confirmed the validity of assumed symmetry. Starting at the UHF level, geometry optimizations were carried through a series of increasing electron correlation methods [UMP2 through UMP4(SDQ)]; density functional theory methods (UB3LYP)[15] were employed to project hyperfine coupling parameters.

The regiochemistry and progression of nucleophilic capture of the vinylcyclopropane radical cation was modeled by placing a CH_3OH molecule within 2.5 Å of the fully optimized structure of *anti*-$\mathbf{1}^{\bullet+}$ while carrying out a transition state geometry optimization at the UHF level followed by a frequency analysis. As for semiempirical methods (PM3) recently used for related systems,[23] preliminary attempts failed to locate transition state structures. Methanol was consistently repelled by the cyclopropane ring, whereas approach to the vinyl function resulted in a range of counterintuitive and experimentally unprecedented structures.

Results

Irradiation of an acetonitrile/methanol (3/1 by volume) solution containing 1,4-dicyanobenzene, phenanthrene, and vinylcyclopropane for ~65 h (~100% consumption) leads to the formation of three ring-opened adducts bearing methoxy as well as *p*-cyanophenyl groups, viz., 3-(*p*-cyanophenyl)-5-methoxy-1-pentene, **2** (38%), (*E*)-1-(*p*-cyanophenyl)-5-methoxy-2-pentene, **3** (34%), and (*E*)-5-(p-cyanophenyl)-1-methoxy-2-pentene, **4** (12%). A fourth product, formed in <2% yield, was not isolated.

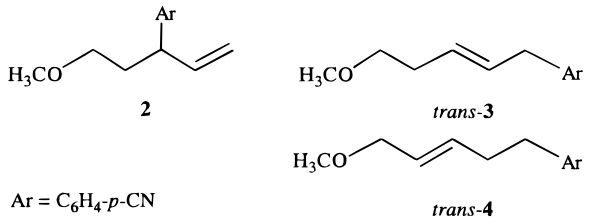

The structure of **2** rests on the presence of 3 olefinic protons, H-1trans (δ 5.08 ppm, dd, 16.9, ~5 Hz), H-1cis (δ 5.11 ppm, dd, 10.3, ~ 5 Hz), and H-2 (δ 5.905 ppm, ddd, 16.9,10.3,7.4 Hz), indicative of a terminal vinyl group. In addition to the benzylic-allylic H-3 (δ 3.55 ppm, ddd, 7.4, 7.4, 7.4 Hz, "q"), there are the complex multiplets of two sets of diastereotopic protons, H-4 (δ 1.965 ppm, 2dddd, 2H) and H-5 (δ 3.29 ppm, 2dddd, 2H), which is further obscured by the methoxy signal at the same chemical shift.

Product **3** is characterized by 2 olefinic protons, H-2 (δ 5.6 ppm, dt, Hz) and H-3 (δ 5.58 ppm, dt, Hz), 2 allylic protons, H-4 (δ 2.33 ppm, dt, Hz, "q"), as well as 2 benzylic protons, H-1 (δ 3.39 ppm, d, Hz), and 2 alkoxy protons, H-5 (δ 3.44 ppm, dt, Hz).

Product **4** shows 2 allylic-alkoxy protons, H-1 (δ 3.85 ppm, d, 5.2 Hz), two olefinic protons, H-2 (δ 5.56 ppm, dt, 15.2, 5.2 Hz) and H-3 (δ 5.71 ppm, dt, 15.2, 5.8 Hz), in addition to two allylic and two benzylic protons, H-4 (δ 2.39 ppm, dt, 7.8, 5.8 Hz, "q") and H-5 (δ 2.78 ppm, t, 7.8 Hz), respectively.

Discussion

Cyclopropane Radical Cations. The structures of cyclopropane radical cationic systems can be viewed as the result of interactions between the frontier molecular orbitals (FMO) of cyclopropane and the substituent. MO calculations suggest that the vertical ionization of cyclopropane occurs from a degenerate pair of in-plane e′ orbitals (**s**, **a**) resulting in a doubly degenerate $^2\mathbf{E}'$ state;[24] first-order Jahn−Teller distortion leads to two nondegenerate electronic states, $^2\mathbf{A_1}$ and $^2\mathbf{B_2}$ (C_{2v} symmetry).[24] The $^2\mathbf{A_1}$ component (orbital **s** singly occupied) relaxes to a "one-electron-bonded trimethylene" structure (type **A**) with one lengthened (but not broken) C−C bond. CIDNP[25a,b,26] or ESR evidence[27] has shown structure type **A** to be predominant for cyclopropane radical cations, including most substituted vinylcyclopropane radical cations.[12a]

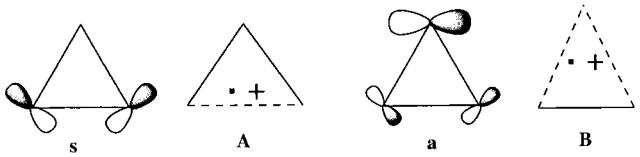

In the alternative $^2\mathbf{B_2}$ component the antisymmetrical molecular orbital **a** is singly occupied. The resulting structure has two lengthened C−C bonds; its cyclopropane fragment resembles a "π-complex" (type **B**).[1e,2a,b,f,25] Structure type **B** is rare; it was first documented in a norcaradiene derivative, where the homoconjugation between the (antisymmetrical) butadiene FMO stabilizes the antisymmetrical cyclopropane FMO.[25b] FMO considerations suggest that structure type **B** can be stabilized also by substitution at a single carbon.[20g] Although 1-methyl- and 1,1-dimethylcyclopropane radical cations were found to undergo distortion to a nonsymmetric structure,[24g] π-substituents such as vinyl or phenyl are expected to stabilize type **B**.

Indeed, the photoelectron spectrum of **1** shows three low-lying bands (9.2, 10.7, and 11.7 eV); two of these were assigned to ionization from molecular orbitals (MOs) resulting from the symmetrical (11.7 eV) and antisymmetrical (9.2 eV) combination of the ethene and the type **B** cyclopropane MO (Figure 1).[28] In this paper, we establish the vinylcyclopropane radical cation ($\mathbf{1}^{\bullet+}$) as the simplest representative of this structure type. Previously, a type **B** structure was assigned to the phenylcyclopropane radical cation based on DFT calculations.[23]

Nucleophilic Capture. Substrates containing alkene or strained-ring moieties may quench suitable photoexcited electron acceptors by electron transfer, generating radical ion pairs. We have used an electron acceptor/sensitizer (1,4-dicyanobenzene) paired with a co-sensitizer (phenanthrene). Arnold and co-workers found that the co-sensitizer improves the yields of electron-transfer photochemical reactions even in cases where electron transfer from the substrate to phenanthrene radical cation is endergonic.[29] The resulting radical cations may be

(23) Dinnocenzo, J. P.; Zuilhof, H.; Lieberman, D. R.; Simpson, T. R.; McKechney, M. W. *J. Am. Chem. Soc.* **1997**, *119*, 994−1004.

(24) (a) Haselbach, E. *Chem. Phys. Lett.* **1970**, *7*, 428. (b) Rowland, C. G. *Chem. Phys. Lett.* **1971**, *9*, 169. (c) Collins, J. R.; Gallup, G. A. *J. Am. Chem. Soc.* **1982**, *104*, 1530. (d) Bouma, W. J.; Poppinger, D.; Radom, L. *Isr. J. Chem.* **1983**, *23*, 21. (e) Wayner, D. D. M.; Boyd, R. J.; Arnold, D. R. *Can. J. Chem.* **1985**, *63*, 3283. Wayner, D. D. M.; Boyd, R. J.; Arnold, D. R. *Can. J. Chem.* **1983**, *61*, 2310. (f) Du, P.; Hrovat, D. A.; Borden, W. T. *J. Am. Chem. Soc.* **1988**, *110*, 3405. (g) Krogh-Jespersen, K.; Roth, H. D. *J. Am. Chem. Soc.* **1992**, *114*, 8388−8394.

(25) (a) Haddon, R. C.; Roth, H. D. *Croat. Chem. Acta* **1984**, *57*, 1165. (b) Roth, H. D.; Schilling, M. L. M. *Can. J. Chem.* **1983**, *61*, 1027. (c) Roth, H. D. *Acc. Chem. Res.* **1987**, *20*, 343−350.

(26) (a) Roth, H. D.; Schilling, M. L. M. *J. Am. Chem. Soc.* **1980**, *102*, 7956−7958. (b) Roth, H. D.; Schilling, M. L. M. *J. Am. Chem. Soc.* **1983**, *105*, 6805−6811.

(27) (a) Iwasaki, M.; Toriyama, K.; Nunome, K. *J. Chem. Soc., Chem. Commun.* **1983**, 202. (b) Qin, X. Z.; Snow, L. D.; Williams, F. *J. Am. Chem. Soc.* **1984**, *106*, 7640−7641. (c) Qin, X. Z.; Williams, F. *Tetrahedron* **1986**, *42*, 6301−6313.

(28) (a) Gleiter, R.; Heilbronner, E.; De Meijere, A. *Helv. Chim. Acta* **1971**, *54*, 1029−1037. (b) Gleiter, R. *Top. Curr. Chem.* **1980**, *86*, 197−285.

(29) (a) Arnold, D. R.; Snow, M. S. *Can. J. Chem.* **1988**, *66*, 3012. (b) Arnold, D. R.; Du, X. *J. Am. Chem. Soc.* **1989**, *111*, 7666.

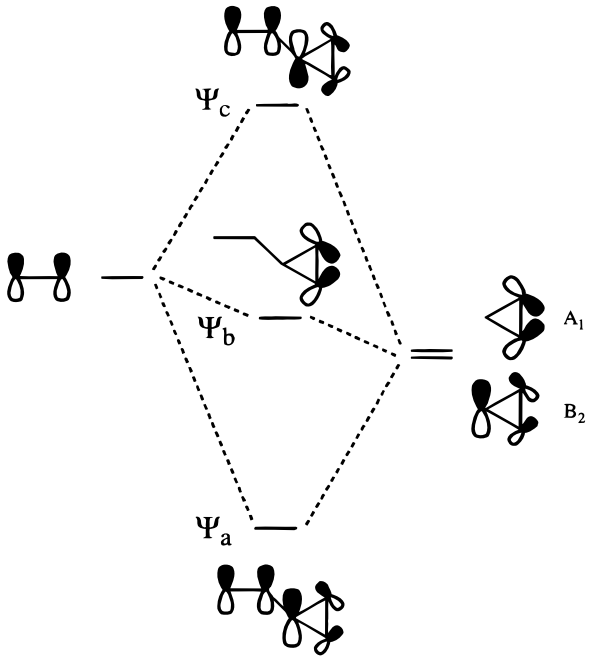

Figure 1. Interaction diagram between the highest occupied orbitals of ethene and cyclopropane (adapted from ref 28b).

captured even by nucleophiles as weak as methanol.[7,10,30] Substrates having both alkene and cyclopropane rings form radical cations in which spin and charge are delocalized between both moieties.[10,12,30]

Irradiating a sensitizer-*co*-sensitizer pair in the presence of a donor (**D**) and a nucleophile (CH_3OH) initiates a well-established photochemical reaction sequence,[7a,9b] generating radical ion pairs ($\mathbf{D}^{\bullet+}$, $\mathbf{DCB}^{\bullet-}$; eq 1). Energetic considerations[31] suggest that the excited-state energy of **DCB** ($E_{(0,0)} = 4.29$ eV)[33] renders electron transfer from **1** ($E_{(D/D^+)} = \sim 2.5$ V)[34] to ^{1}**DCB*** ($E_{(A^-/A)} = -1.6$ V;[37] $^*E_{(A^-/A)} = 2.7$ V) moderately exergonic ($\Delta G = -0.2$ eV). Subsequent nucleophilic capture of $\mathbf{1}^{\bullet+}$ ($\mathbf{D}^{\bullet+}$) by methanol (eq 2) and reaction of the methoxy-substituted free radical ($^{\bullet}\mathbf{D}-OCH_3$) with the radical anion ($\mathbf{DCB}^{\bullet-}$) by aromatic substitution (eq 3) can account for all isolated products. The fact that all products contain the methoxy group is evidence for the formation of the radical cation and its nucleophilic capture.

$$\mathrm{Ph} + \mathrm{DCB} + \mathrm{D} \xrightarrow{h\nu} \mathrm{Ph} + \mathrm{DCB}^{\bullet-} + \mathrm{D}^{\bullet+} \qquad (1)$$

$$\mathrm{D}^{\bullet+} + \mathrm{CH_3OH} \rightarrow {}^{\bullet}[\mathrm{D}-\mathrm{OCH_3}] + \mathrm{H}^+ \qquad (2)$$

$$^{\bullet}[\mathrm{D}-\mathrm{OCH_3}] + \mathrm{DCB}^{\bullet-} \rightarrow p\text{-CN-C}_6\mathrm{H}_4-\mathrm{D}-\mathrm{OCH_3} + \mathrm{CN}^- \qquad (3)$$

The nucleophilic capture of a vinylcyclopropane system can illuminate several diverse aspects: (1) the regiochemistry of the reaction probes how the delocalization of spin and charge is reflected in the reactivity pattern of the radical cation; (2) for rotationally mobile radical cations, e.g., chrysanthemol[30] or vinylcyclopropane (discussed here), the geometry of the reaction products reflects the conformation of the vinyl group relative to the cyclopropane moiety in the radical cation; (3) for rigid radical cations (e.g., bicyclo[3.1.0]hex-2-ene,[12a] sabinene, α- or β-thujene),[10] the stereochemistry of the methoxy group in the products delineates the approach of the nucleophile.

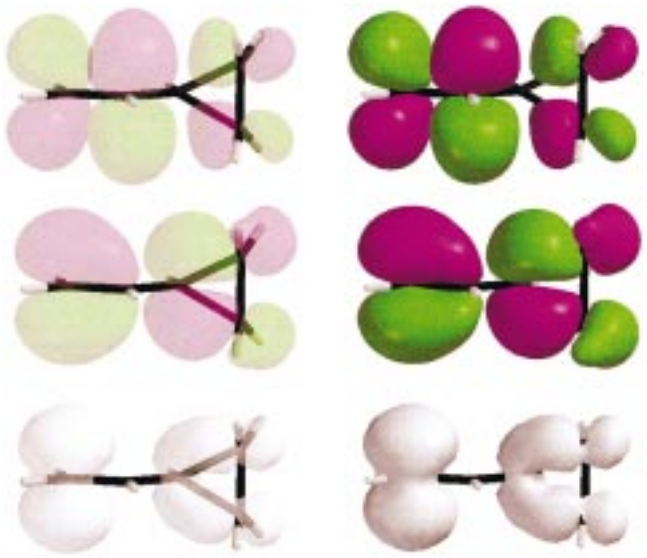

Figure 2. Spartan representation of unpaired spin density (bottom), SOMO (center), and LUMO (top) for the vinylcyclopropane radical cation.

Regiochemistry of Nucleophilic Capture. The orbital coefficients of radical cation SOMOs and LUMOs have been invoked to explain the regio- and stereochemistry of nucleophilic capture for these species; nucleophiles preferentially attack carbons with significant coefficients at both SOMO and LUMO.[38−42] Spartan representations of SOMO and LUMO of $\mathbf{1}^{\bullet+}$ (Figure 2)[43] suggest that attack is feasible at both cyclopropane and vinyl function. Attack at a secondary cyclopropane carbon is expected to yield an allylic radical, $\mathbf{5}^{\bullet}$; this process can be rationalized as a nucleophilic substitution with a carbon-centered free radical as an intramolecular leaving group.[7,10] Attack at the vinyl group ("addition" to the alkene function) would form either the cyclopropylcarbinyl species, $\mathbf{6}^{\bullet}$, or the (rearranged) primary radical, $\mathbf{7}^{\bullet}$; the latter process has precedent in the (intramolecular) capture of chrysanthemol radical cation. Coupling of $\mathbf{5}^{\bullet}$ with the sensitizer radical anion, $\mathbf{DCB}^{\bullet-}$, is expected to result in the formation of **2** and **3**, whereas coupling of $\mathbf{7}^{\bullet}$ with $\mathbf{DCB}^{\bullet-}$ would produce **4**. Neither the structure of the substrate nor that of the products provide a criterion for the stereochemistry of the approach of the nucleophile.

(30) Herbertz, T.; Roth, H. D. *J. Am. Chem. Soc.* **1996**, *118*, 10954−10962.
(31) The free energy of electron transfer was calculated according to the Rehm−Weller equation, $-\Delta G = E_{(0,0)} - E_{(D/D^+)} + E_{(A^-/A)} + e^2/\epsilon a$.[32]
(32) (a) Knibbe, H.; Rehm, D.; Weller, A. *Ber. Bunsen-Ges. Phys. Chem.* **1968**, *72*, 257. (b) Weller, A. *Pure Appl. Chem.* **1968**, *16*, 115. (c) Rehm, D.; Weller, A. *Isr. J. Chem.* **1970**, *8*, 259.
(33) Arnold, D. R.; Maroulis, A. J. *J. Am. Chem. Soc.* **1976**, *98*, 5931.
(34) The oxidation potential of **1** is estimated at 2.5 V from its ionization potential (IP = 9.2 eV)[28] and the empirical equation[35] $E_{(D/D^{\bullet+})} = 0.92 \times (IP) - 6.2$; it should also lie below that of 1,3-butadiene (2.7 V).[36]
(35) Miller, L. L.; Nordblom, G. D.; Mayeda, E. A. *J. Org. Chem.* **1972**, *37*, 916−918.
(36) McManus, K. A.; Arnold, D. R. *Can. J. Chem.* **1994**, *72*, 2291−2304.
(37) Mattes, S. L.; Farid, S. *Org. Photochem.* **1983**, *6*, 233.
(38) Pross, A. *J. Am. Chem. Soc.* **1986**, *108*, 3537.
(39) Shaik, S. S.; Pross, A. *J. Am. Chem. Soc.* **1989**, *111*, 4306.
(40) (a) Eberson, L.; Radner, F. *Acta Chem. Scand.* **1992**, *46*, 312. (b) Eberson, L.; Radner, F. *Acta Chem. Scand.* **1992**, *46*, 802. (c) Eberson, L.; Hartshorn, M. P.; Radner, F.; Merchan, M.; Roos, B. O. *Acta Chem. Scand.* **1993**, *47*, 176.
(41) (a) Shaik, S. S.; Dinnocenzo, J. P. *J. Org. Chem.* **1990**, *55*, 3434. (b) Shaik, S. S.; Reddy, A. C.; Ioffe, A.; Dinnocenzo, J. P.; Danovich, D.; Cho, J. K. *J. Am. Chem. Soc.* **1995**, *117*, 3205−3222.
(42) Herbertz, T.; Blume, F.; Roth, H. D. *J. Am. Chem. Soc.* **1998**, *120*, 4591−4599.
(43) SPARTAN, SGI Version 4.0.4 GL, Wave function Inc., 1991−1995, Irvine, CA; Deppmeier, B. J., Driessen, A. J., Hehre, W. J., Johnson, H. C., Leonard, J. M., Yu, J., Lou, L., Development Staff; Baker, J., Carpenter, J. E., Dixon, R. W., Fielder, S. S., Kahn, S. D., Pietro, W. J., Contributors.

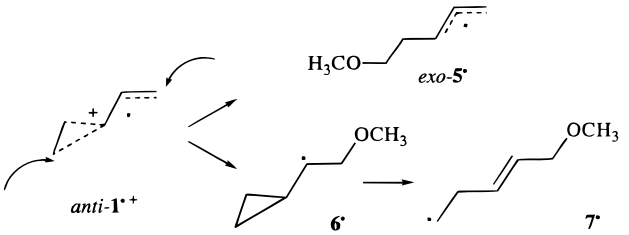

The attack of methanol on $\mathbf{1}^{\bullet+}$ is regioselective: attack at one of the ring carbons is favored 6:1 over attack at the vinyl group. This result is surprising in view of the fact that several substituted vinylcyclopropane radical cations, including those of sabinene,[10a] α-thujene,[10b] and 2-carene,[12b] are attacked in regiospecific fashion at the most highly substituted cyclopropane carbon. The lack of regiospecificity encountered for $\mathbf{1}^{\bullet+}$ sets this species apart from other vinylcyclopropane radical cations studied so far.[7,10,12,23,30] All these species showed a high degree of regiospecificity. The reduced regiospecificity of $\mathbf{1}^{\bullet+}$ may reflect the inherent reactivity of the unusual structure (type **B**) of the cyclopropane moiety; these aspects are discussed below with the ab initio calculations. Alternatively, the reason for the attack on the vinyl group may be rooted in the energetics of electron transfer. Since the reaction of **1** with ^{1}**DCB*** is only modestly exergonic, it may form contact radical ion pairs or excited-state complexes, in which the sensitizer radical anion may somewhat divert the nucleophilic attack.

Conformation of Vinylcyclopropane Radical Cation. The geometry of the newly formed double bond of free radical **5**• (and product **3**) is of interest because it may reflect the preferred conformation of the vinyl group relative to the cyclopropane moiety in the radical cation, $\mathbf{1}^{\bullet+}$. Capture of *anti*-$\mathbf{1}^{\bullet+}$ is expected to form *exo*-**5**•, whereas trapping of *syn*-$\mathbf{1}^{\bullet+}$ should produce *endo*-**5**•. Subsequent aromatic substitution of the isomers of **5**• on the acceptor radical anion, $\mathbf{DCB}^{\bullet-}$, should occur preferentially at the terminal carbons of the allyl radicals, yielding different isomers of **3**; *exo*-**5**• is expected to form *trans*-**3** whereas the reaction of *endo*-**5**• would generate *cis*-**3**. Attack of C3 on $\mathbf{DCB}^{\bullet-}$ would yield the terminal olefin, **2**, from both allyl radicals. Related arguments were advanced in connection with the intramolecular capture of chrysanthemol radical cation.[30]

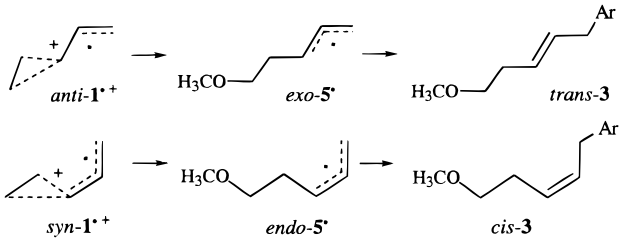

The results support the preferential (or exclusive) capture of *anti*-$\mathbf{1}^{\bullet+}$. The ratio of *trans*-**3** to *cis*-**3** is ∼20:1, if the minor, unidentified product (vide supra) is *cis*-**3**; otherwise, it is even higher. The populations of the isomeric radical ions, *anti*- and *syn*-$\mathbf{1}^{\bullet+}$, should be dictated by the populations of the trans and gauche conformers of **1**, i.e., ∼3:1.[20a] Because of their short lifetimes, no interconversion between *anti*- and *syn*-$\mathbf{1}^{\bullet+}$ is expected. In light of these considerations, the high ratio of *trans*- to *cis*-**3** may indicate that the nucleophilic capture of *syn*-$\mathbf{1}^{\bullet+}$ at the cyclopropane function is retarded.

Ab Initio Calculations

To further illuminate our experimental results concerning the structural features of vinylcyclopropane radical cation and the regiochemistry of its nucleophilic capture we carried out various ab initio calculations. The results for the radical cation are viewed relative to the parent molecule. Our calculations on the potential energy surface of **1** at the RMP2/6-31G* level are in good agreement with the majority of previous studies.[21] We confirmed the existence of *s*-*anti*-**1** and *s*-*gauche*-**1** minima (Figure 3); *s*-*gauche*-**1** (C_1 symmetry; dihedral angle Cβ−Cα−C1−midpoint C2,C3 = ±57°) lies 0.98 kcal/mol higher in energy than *s*-*anti*-**1** (C_s symmetry; dihedral angle 180°). At 273 K this energy difference corresponds to an equilibrium constant, *K*, of 6.3 between *anti* and *gauche* conformers. The syn conformer (C_s symmetry; dihedral angle 0°) is a transition state, 0.78 kcal/mol above the gauche conformers.

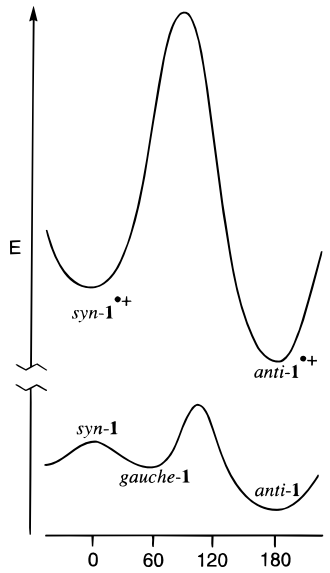

Figure 3. Comparison of potential energy diagrams for rotation around the C1−Cα bond of vinylcyclopropane (bottom) and its radical cation (top).

Table 1. Computed Energy Differences (kcal/mol) between Conformers of $\mathbf{1}^{\bullet+}$

level of theory	HF	B3LYP	MP2	MP3	MP4SDQ
$\Delta E_{anti-syn}$	3.15	3.00	2.81	2.76	2.81

Vinylcyclopropane Radical Cation. The potential surface of the radical cation, $\mathbf{1}^{\bullet+}$ (Figure 3), has a different topology from that of the parent. Radical cations with dihedral angles, Cβ−Cα−C1−midpoint C2,C3, near that of the gauche conformer of **1** relax to the syn structure. The syn conformer is a minimum, lying ∼3 kcal/mol above *s*-*anti*-$\mathbf{1}^{\bullet+}$. The energy difference between *anti* and *syn* conformers (and the structure parameters) depends on the degree of electron correlation included in the calculation. The results at any level of theory indicate an increased free energy difference (>1 kcal/mol) between the two minima, *s*-*anti*-$\mathbf{1}^{\bullet+}$ and *s*-*syn*-$\mathbf{1}^{\bullet+}$ (Table 1). The increase can be rationalized on the basis of MO considerations. Removal of an electron from the HOMO of **1** (Ψ_c, Figure 1),[28] which is antibonding between C_1 and C_α, results in a shorter, stronger bond and in increased nonbonding H−H interactions between the terminal vinyl and the secondary cyclopropane hydrogens (Figure 4). Similar considerations suggest an increased barrier to rotation about the C_1-C_α bond.

The results for **1** and $\mathbf{1}^{\bullet+}$ show similar trends as those for 1,3-butadiene, **8**,[45,46] and its radical cation.[44] 1,3-Butadiene also

(44) (a) Aebischer, J. N.; Bally, T.; Roth, K.; Haselbach, E.; Gerson, F.; Qin, X.-Z. *J. Am. Chem. Soc.* **1989**, *111*, 1909−1914. (b) Wiest, O. *J. Am. Chem. Soc.* **1997**, *119*, 5713−5719.

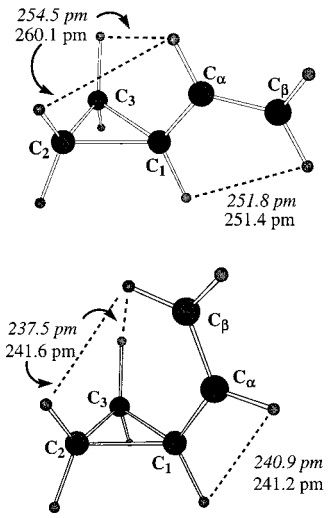

Figure 4. Comparison of H−H nonbonding interaction distances of the s-syn and s-anti conformers of vinylcyclopropane (Roman type) and its radical cation (italics).

Table 2. Computed Energy Differences (MP2/6-31G*) and Estimated Barrier Heights between Parent and Radical Cation Conformers of **1** and **8**

system	$\Delta E_{anti-syn}$ (kcal/mol)	$\Delta H^{\ddagger}$ (kcal/mol)
1	1.76	3−4
1$^{\bullet+}$	2.76	13−17
8	3.57	5−6
8$^{\bullet+}$	4.19	20−25

has an s-trans (C_{2h} symmetry) and two equivalent gauche conformers (C_1) ∼0.1−0.5 kcal/mol below an s-cis (C_{2v}) transition state. The potential surface of **8**$^{\bullet+}$ again is different from that of **8**; a *trans*-**8**$^{\bullet+}$ (C_{2h}) lies ∼3−4 kcal/mol below *s-cis*-**8**$^{\bullet+}$ (C_{2v}); the barrier to rotation is estimated to amount to 20−25 kcal/mol (Table 2).[44a] The rotational barriers of **8**$^{\bullet+}$ and **1**$^{\bullet+}$ are significantly increased compared to those of **8** and **1**, respectively. The more than 5-fold increase of the rotational barrier of **8**$^{\bullet+}$ vs **8** is ascribed to a reduced antibonding interaction across C2−C3 in the SOMO of **8**$^{\bullet+}$ and, consequently, increased double bond character. The increased barrier for **1**$^{\bullet+}$ vs **1** is explained similarly; the antibonding interaction between C1−Cα in the HOMO is reduced in the SOMO, resulting in an increased bonding interaction for **1**$^{\bullet+}$ (Figure 1).

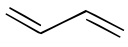

8

Although we have calculated both conformers, we limit our comments to the (more stable) *s-anti*-**1**$^{\bullet+}$ (Table 3), because the calculated (UMP2/6-31G*) bond lengths for the two conformers of **1**$^{\bullet+}$ show similar trends. The allylic cyclopropane bonds C1−C2 (C1−C3) are lengthened (+6%) whereas the bond connecting the secondary cyclopropane carbons C2−C3 is shortened (−4%). Also, the distinct difference between the (vinyl) double bond (134.0 pm) and the bond linking cyclopropane and ethene functions (147.5 pm) is diminished; the corresponding bonds are of essentially equal length (139.8). As a result, the array, Cβ−Cα−C1, has been converted to an allyl moiety. Overall, *s-anti*-**1**$^{\bullet+}$ and *s-syn*-**1**$^{\bullet+}$ have structures of type **B**; they resemble an allyl function interacting with an ethene molecule.

Table 3. Calculated Bond Lengths (pm) of *anti*-Vinylcyclopropane and Its Radical Cation

	anti-**1**$^{\bullet+}$					
bond	HF	B3LYP	MP2	MP3	MP4	*anti*-**1** MP2
C1−C2	162.1	162.5	160.3	161.0	161.2	151.3
C2−C3	141.9	143.5	143.6	143.5	143.5	149.8
C1−Cα	138.7	140.6	140.1	139.9	140.1	147.5
Cα−Cβ	140.0	139.3	139.6	139.7	139.8	134.0

The spin densities calculated for the two conformers (Table 4) reflect the conclusions derived from the bond lengths; most of the unpaired electron density is located on the tertiary cyclopropane carbon (C1) and the terminal vinyl carbon (Cβ). Calculations with UB3LYP//UB3LYP and UMP2//UB3LYP methodologies, respectively, show only minor differences. The general type of spin density distribution calculated for the two conformers of **1**$^{\bullet+}$ has precedent in several vinylcyclopropane systems with "locked" geometries, including the radical cations of sabinene and its simplified model, 2-methylenebicyclo[3.1.0]-hexane,[10c] as well as that of bicyclo[3.1.0]hex-2-ene.[10c,12a]

The major hyperfine coupling constants (hfc) are related to the spin densities by one of two different mechanisms. ^{1}H nuclei attached to a carbon with electron spin density interact by $\pi-\sigma$-spin polarization (yielding a negative hfc); ^{1}H nuclei one C−C bond removed from such a carbon are coupled by $\pi-\sigma$-delocalization (hyperconjugation; yielding a positive hfc). Accordingly, the terminal vinylic ^{1}H nuclei and the allylic cyclopropane protons have strong negative hfcs whereas the secondary cyclopropane protons have significant positive hfcs. The secondary cyclopropane protons show interesting stereoelectronic effects: large hfcs are calculated for the anti nuclei whereas small or negligible hfcs are found for the syn protons. These predictions are reminiscent of experimental (CIDNP) results observed for the corresponding nuclei of bicyclo[3.1.0]-hex-2-ene (**9**) during the electron-transfer reaction with chloranil.[12a] In general, UB3LYP calculations on UB3LYP or UMP2 geometries give very similar results (Table 4).

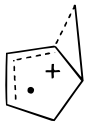

9$^{\bullet+}$

Of course, the comparison between **9**$^{\bullet+}$ and *syn*-**1**$^{\bullet+}$ may be flawed because the rigid geometry of **9**$^{\bullet+}$ imposes a dihedral angle (∼30°) noticeably different from the 0° of *syn*-**1**$^{\bullet+}$, causing the three-membered rings of **9**$^{\bullet+}$ and *syn*-**1**$^{\bullet+}$ to have different symmetries. To allow a more meaningful comparison between the two species, we analyzed the structural features of a conformer of *syn*-**1**$^{\bullet+}$ with an imposed dihedral angle of 30°. This conformer reproduced the stereoelectronic effect that causes the lateral (C1−C6) bond of **9**$^{\bullet+}$ to be primarily involved in delocalizing spin and charge. The calculated bond lengths for the cyclopropane function of **9**$^{\bullet+}$ match those of the *syn*-**1**$^{\bullet+}$ conformer with "arrested" dihedral angle (Figure 5).

In view of the changes in bond lengths and bond angles in *syn*-**1**$^{\bullet+}$ with a specific dihedral angle imposed, we probed the dependence of these parameters on the dihedral angle (Cβ−Cα−C1−midpoint C2,C3) over the full range of rotation. The resulting changes in bond distances and cyclopropane bond angles as a function of imposed dihedral angle demonstrate the

(45) Olivucci, M.; Ragazos, I. N.; Bernadi, F.; Robb, M. A. *J. Am. Chem. Soc.* **1993**, *115*, 3710−3721.
(46) Murcko, M. A.; Castejon, H.; Wiberg, K. B. *J. Phys. Chem.* **1996**, *100*, 16162−16168.

Table 4. Diagonal Terms of Atomic−Atomic Spin Densities (ρ) and Calculated Hyperfine Coupling Constants (G)[a] for *anti*-**1**$^{\bullet+}$

anti-**1**$^{\bullet+}$	HF $S^2 = 0.820$	B3LYP//B3LYP $S^2 = 0.760$	B3LYP//MP2 $S^2 = 0.760$	MP2//MP2 $S^2 = 0.809$	MP3 $S^2 = 0.813$	MP4 $S^2 = 0.814$
C1	0.264	0.231	0.215	0.216	0.221	0.224
(H1)	*(−10.67)*	*(−6.20)*	*(−5.83)*	*(−9.23)*	*(−9.39)*	*(−9.54)*
C2	0.134	0.130	0.127	0.133	0.134	0.134
($H2_{syn}$, $H2_{anti}$)	*(−1.30, 5.18)*	*(0.50, 7.10)*	*(0.32, 7.63)*	*(−1.54, 5.45)*	*(−1.61, 5.64)*	*(−1.59, 5.63)*
Cα	−0.187	0.013	0.018	−0.132	−0.139	−0.144
(Hα)	*(5.61)*	*(−1.00)*	*(−0.63)*	*(3.67)*	*(3.94)*	*(4.13)*
Cβ	0.870	0.577	0.592	0.848	0.851	0.853
($H\beta_{syn}$, $H\beta_{anti}$)	*(−33.12, −34.12)*	*(−14.60, −15.00)*	*(−15.51, −15.94)*	*(−32.88, −33.70)*	*(−32.98, −33.86)*	*(−33.08, −33.93)*

[a] Given in italic type; obtained by multiplying the Fermi contact term (FCT) with a proportionality factor of 1596 G au^{-1} (*Exploring Chemistry with Electronic Structure Methods*, 2nd ed.; Gaussian Inc, 1996; p 136).

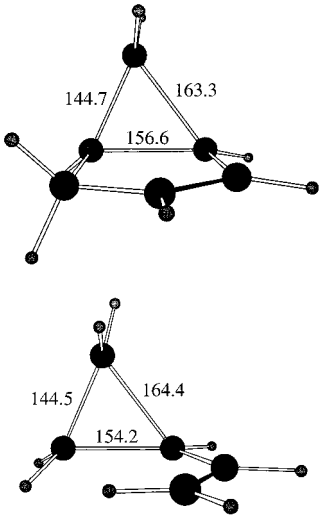

Figure 5. Comparison of bicyclo[3.1.0]hex-2-ene and *syn*-vinylcyclopropane radical cations (30° dihedral angle).

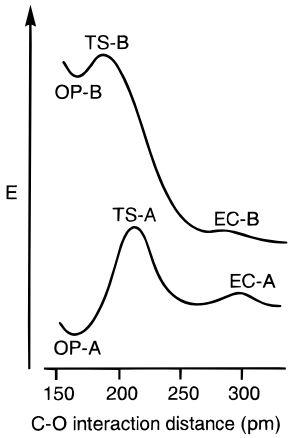

Figure 6. Schematic reaction profiles for nucleophilic capture of *anti*-**1**$^{\bullet+}$ at C3 (path **A**; bottom) and Cβ (path **B**; top). See Table 5 for actual energy differences.

significance of stereoelectronic effects for the structure of **1**$^{\bullet+}$. Even small deviations from 0° and 180° cause significant changes in the bond lengths and angles of the cyclopropane function.

Transition States for Nucleophilic Capture. Calculations modeling the capture of **1**$^{\bullet+}$ by methanol were carried out by ab initio methods at the UHF/6-31G* level of theory. Several authors have compared experimental results to data calculated with ab initio methods, both without (HF) and with electron-correlation (MP2), and including density functional theory (DFT) methods.[47−56] These comparisons suggest that structural features are more sensitive to the size of the basis set than to the method used. Hence, we restricted our transition state geometry optimizations to the UHF/6-31G* level of theory and UB3LYP/6-31G* single-point calculations.

The capture of the cyclopropane radical cation by various nucleophiles was studied recently by ab initio calculations.[41] This reaction (modeled without solvent) is characterized by three extrema: an encounter complex (**EC**) precedes the actual transition state (**TS**) leading to an oxonium (**OP**) and a free radical "product", for capture by an alcohol and an anion, respectively. For the nucleophilic capture of *trans*-**1**$^{\bullet+}$ by methanol our calculations identified two reaction pathways, featuring attack at either one secondary cyclopropane carbon (path **A**) or the terminal vinylic carbon (path **B**). Details of the pathways were studied by carrying out partial geometry optimizations (UHF/6-31G*) with fixed C−O distances in 5−10 pm increments. The reaction profiles are similar, in principle, but the energetics of the two pathways are markedly different (Figure 6).

The attack on the cyclopropane function proceeds toward ring opening, with an allyl radical as an emerging intramolecular leaving group (**TS-A**; Figure 7); this capture proceeds in "typical" S_N2 fashion, causing encounter complex (**EC-A**) and transition state to be relatively early. Attack on the cyclopropane moiety is firmly supported by experimental evidence in a range of systems.[7,10,23,30] The second mode of attack involves the terminal vinyl carbon (C$_\beta$), foreshadowing a cyclopropylcarbinyl intermediate. In this case, the lateral cyclopropane bonds begin to contract as methanol approaches the vinyl function (**TS-B**; Figure 8). The need of Cβ to undergo rehybridization leads to a later, more "product-like" transition state.

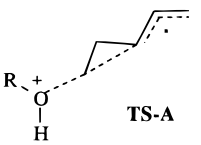

TS-A

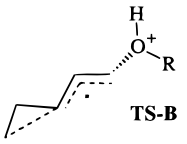

TS-B

(47) Bottoni, A. *J. Chem. Soc., Perkin Trans. 2* **1996**, 2041−2047.
(48) Ventura, O. N.; Kieninger, M.; Coitino, E. L. *J. Comput. Chem.* **1996**, *17*, 1309−1317.
(49) Nowek, A.; Leszczynski, J. *J. Chem. Phys.* **1996**, *104*, 1441−1451.
(50) Mole, S. J.; Zhou, X.; Liu, R. *J. Phys. Chem.* **1996**, *100*, 14665−14671.
(51) Andrés, J.; Moliner, V.; Safont, V. S.; Domingo, L. R.; Picher, M. T. *J. Org. Chem.* **1996**, *61*, 7777−7783.
(52) Hertwig, R. H.; Koch, W. *J. Comput. Chem.* **1995**, *16*, 576−585.
(53) Bauschlicher, C. W., Jr. *Chem. Phys. Lett.* **1995**, *246*, 40−44.
(54) Johnson, B. G.; Gonzales, C. A.; Gill, P. M. W.; Pople, J. A. *Chem. Phys. Lett.* **1994**, *221*, 100−108.
(55) Wiest, O.; Black, K. A.; Houk, K. N. *J. Am. Chem. Soc.* **1994**, *116*, 10336−10337.
(56) Fan, L.; Ziegler, T. *J. Am. Chem. Soc.* **1992**, *114*, 10890.

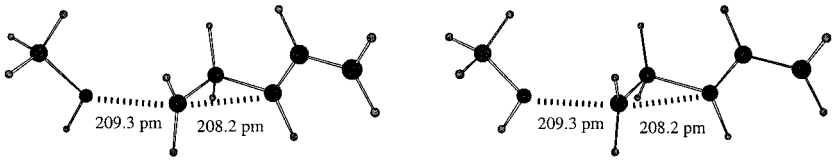

Figure 7. Transition state (stereoview) for the nucleophilic capture of vinylcyclopropane radical cation by methanol at the secondary cyclopropane carbon.

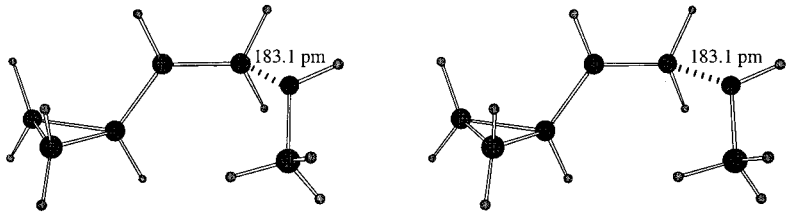

Figure 8. Transition state (stereoview) for the nucleophilic capture of the vinylcyclopropane radical cation by methanol at the vinyl carbon.

Table 5. Calculated Energies Relative to EC-A (kcal/mol), Bond Lengths (pm), and Encounter Distances (pm) for Encounter Complexes (ECs), Transition States (TSs), and Oxonium Ions (OPs)

Attack at C3			
bond	EC-A	TS-A ΔE(UHF) = 1.48	OP-A ΔE(UHF) = −10.90
C3−O	295.9	209.3	151.8
C1−C3	179.9	208.2	245.5
C1−C2	152.2	151.8	150.8
C2−C3	144.3	145.5	151.7

Attack at Cβ			
bond	EC-B ΔE(UHF) = 2.04	TS-B ΔE(UHF) = 9.96	OP-B ΔE(UHF) = 8.40
Cβ−O	279.0	183.1	156.7
C1−C3	161.2	153.2	152.5
C1−C2	157.6	152.6	151.5
C2−C3	143.1	147.1	148.0

TS-A has two partial bonds of similar length (Table 5; C3−O 209.3 pm, C1−C3 208.2 pm), whereas the developing C2−O bond in **TS-B** is significantly shorter (183.1 pm) (cf. the capture of norcaradiene radical cation).[42] The release of ring strain during attack at C3 leads to a lower lying transition state, compared to addition at the vinyl terminus (Table 5). The energy difference between **TS-A** and **TS-B** of ∼8.5 kcal/mol (HF/6-31G*) is likely overestimated. A much smaller difference (∼1.5 kcal/mol) is obtained upon single-point UB3LYP calculation at the UHF geometry (UB3LYP/6-31G*//UHF/6-31G*). This value shows better agreement with the relative yields of the electron-transfer products [ratio of (**2** plus *trans*-**3**) to *trans*-**4**].[57]

The nucleophilic capture is completed with formation of the oxonium ions. **OP-A** no longer shows any bonding interaction between C1 and C3 whereas **OP-B** still contains a localized cyclopropylcarbinyl function. The strain inherent in the small ring function causes a substantial energy difference between resulting oxonium ions (HF ∼ 19 kcal/mol; B3LYP//HF ∼ 11 kcal/mol).

In summary, our calculations modeling the nucleophilic capture of *trans*-**1**$^{\bullet+}$ are in good agreement with related calculations on cyclopropane and arylcyclopropane radical cations.[23,41] Also, the calculations correctly reproduce the two sites of attack and project relative transition state energies in accord with the observed product distribution.

Conclusion

Products **2**−**4**, generated by electron-transfer photochemistry of vinylcyclopropane (**1**), are rationalized by attack of methanol on the radical cation, **1**$^{\bullet+}$, either at a secondary or the terminal vinylic carbon. The potential surface of **1**$^{\bullet+}$, probed by ab initio calculations, has two minima, *anti*- and *syn*-**1**$^{\bullet+}$; both belong to an unusual structure type with two lengthened cyclopropane bonds. The attack occurs at centers with high orbital coefficients for both SOMO and LUMO. The calculated transition state for nucleophilic capture at the cyclopropane ring lies below that for attack at the vinyl group, in agreement with the observed reactivity. The emerging principles governing the nucleophilic attack on bi- or trifunctional radical cationic systems are being tested and elaborated further on additional substrates with use of experimental and theoretical approaches.

Acknowledgment. Financial support of this work by the National Science Foundation through grants NSF CHE-9414271 and CHE-9714271 and an equipment grant NSF CHE-9107839 is gratefully acknowledged. A generous allocation of supercomputer time from NCSA (CHE980003N) at Urbana−Champaign, Illinois, is also gratefully acknowledged.

Supporting Information Available: Tables giving NMR spectral assignments for products **2**−**4**, Cartesian coordinates and total energies for all calculated species, bond lengths, angles, spin densities, and hyperfine coupling constants for *syn*-**1**$^{\bullet+}$, relative energies and cyclopropane bond lengths and angles of **1**$^{\bullet+}$ as a function of imposed dihedral angle (Cβ−Cα−C1−midpoint C2,C3), bond distances and spin densities for **6**$^{\bullet}$, **7**$^{\bullet}$, and **TS-C**, energy differences between extrema on the potential surface of nucleophilic capture (18 pages, print/PDF). See any current masthead page for ordering information and Web access instructions.

JA980367S

(57) Attempts to locate transition state geometries and energies for TS-A and TS-B at the UB3LYP and UMP2 level were unsuccessful; standard TS optimizations as well as those including the "OPT=CALCHFFC" option suffered from convergence problems, whereas those using the "OPT=CALCALL" option exceeded the allocated supercomputing resources. We intend to revisit this problem by extending the reaction profiles obtained at the UHF level (Figure 6) to the UB3LYP and/or UMP2 levels. In addition, we plan to include solvation approximations in modeling the nucleophilic capture of simple radical cations, such as **1**$^{\bullet+}$.